Food Research International xxx (xxxx) xxx–xxx

Contents lists available at ScienceDirect

Food Research International

journal homepage: www.elsevier.com/locate/foodres

Monitoring molecular composition and digestibility of ripened bresaola through a combined foodomics approach

Gianfranco Picone[a,1], Ivano De Noni[b,1], Pasquale Ferranti[c], Maria Adalgisa Nicolai[c], Cristina Alamprese[b], Alessia Trimigno[a], Andre Brodkorb[d], Reto Portmann[e], Anne Pihlanto[f], Sedef Nehir El[g], Francesco Capozzi[a,h,*]

[a] Department of Agricultural and Food Sciences (DISTAL), University of Bologna, 47521 Cesena, Italy
[b] Department of Food, Environmental and Nutritional Sciences (DeFENS), University of Milan, 20133 Milan, Italy
[c] Department of Agricultural Sciences, University of Naples "Federico II", 80055 Portici, Naples, Italy
[d] Teagasc Food Research Centre, Moorepark, Fermoy, Co. Cork P61 C996, Ireland
[e] Agroscope, Institute for Food Sciences, Schwarzenburgstr. 161, 3003 Bern, Switzerland
[f] Natural Resources Institute Finland (Luke), FI-00790 Helsinki, Finland
[g] Ege University, Food Engineering Department, Nutrition Section, 35040 Bornova-İZMİR, Turkey
[h] Interdepartmental Centre for Industrial Agri-Food Research (CIRI), University of Bologna, 47521 Cesena, Italy

ARTICLE INFO

Keywords:
Bresaola
Meat
In vitro digestion
Peptides
Bioactivity
Proteomics
NMR
Foodomics

ABSTRACT

In this work, the effects of maturation time and simulated gastrointestinal digestion on the molecular and peptide profiles of "Bresaola Valtellina" were assessed through the foodomics approach, in this case food proteomics and peptidomics combined to other analytical and biological assays, aiming at depicting a holistic food quality. Human digestion of this Italian cured meat product was simulated using an *in vitro* static protocol and the degree of proteolysis and the *in vitro* bioactivity of the soluble free compounds in the digestates were evaluated by biochemical assays, *e.g.* SDS-PAGE, size exclusion HPLC, HPLC/MS, ^{1}H NMR, enzymatic and antioxidant activities. The obtained results demonstrated that *in vitro* gastrointestinal digestion contributed to a considerable release of myofibrillar proteins by the muscle tissue. Data from SDS-PAGE, peptidomic and size exclusion HPLC assays showed that the *in vitro* digestion largely degraded proteins of muscle tissue to peptides smaller than 250 Da. The released peptides were likely responsible for the inhibitory activity on amylolytic enzymes and for the antioxidant properties elicited by the gastric digestates of Bresaola. Overall, the results demonstrated the negligible role of ripening in making meat proteins more bioaccessible, whereas they confirmed the highly *in vitro* digestibility of meat proteins from Bresaola. This study represents a new approach merging proteomics and foodomics to evaluate the effect of ripening and *in vitro* digestion on the bioactivity and bioaccessibility of proteins and peptides of meat products.

Abbreviations: AA, Antioxidant Activity; ABTS, 2,2′-azinobis 3-ethylbenzothiazoline-6-sulfonate; ACTS, Actin; ANOVA, Analysis Of Variance; DE, Delay Extraction; DPPH, 1,1-Diphenyl-2-Picrylhydrazyl; ENOB, Beta-Enolase; ESI, Electrospray Ionization; FRAP, Ferric Reducing Antioxidant Power; G3P, glyceraldehyde-3-phosphate dehydrogenase; Gln, Glutamine; HMW, High Molecular Weight; ^{1}H NMR, ^{1}H Nuclear Magnetic Resonance; IC50, 50% inhibition of the initial rate of reaction; KCRM, Creatine Kinase M-type; HPLC, High-Performance Liquid Chromatography; LDHA, L-lactate Dehydrogenase A chain; LMW, Low Molecular Weight; LSD, Least Significant Difference; MALDI TOF, Matrix-Assisted Laser Desorption/Ionization-Time Of Flight; MHC, Myosin Heavy Chain; MLRS, Myosin Regulatory Light Chain; MS, Mass Spectrometry; MW, Molecular Weight; MYH1, Myosin-1; MYL1, Myosin Light Chain; NOESY, Nuclear Overhauser Effect Spectroscopy pulse sequence; nrNCBI, National Center for Biotechnology Information; PGI, Protected Geographical Indication; PMF, Peptide Mass Fingerprinting; PSD, Post-source Decay; SDS-PAGE, Sodium Dodecyl Sulfate Polyacrylamide Gel Electrophoresis; TFA, Trifluoroacetic Acid; TMSP, 3-Trimethylsilyl-Propanoic-2,2,3,3-d4 acid sodium salt; TPA, Texture Profile Analysis; Trolox, (6-hydroxy-2,5,7,8-tetramethylchroman-2-carboxylic acid)

* Corresponding author at: Department of Agricultural and Food Sciences (DISTAL), University of Bologna, 47521 Cesena, Italy.
E-mail address: francesco.capozzi@unibo.it (F. Capozzi).

[1] Both authors contributed equally to this work.

https://doi.org/10.1016/j.foodres.2018.11.021
Received 4 September 2018; Received in revised form 8 November 2018; Accepted 12 November 2018

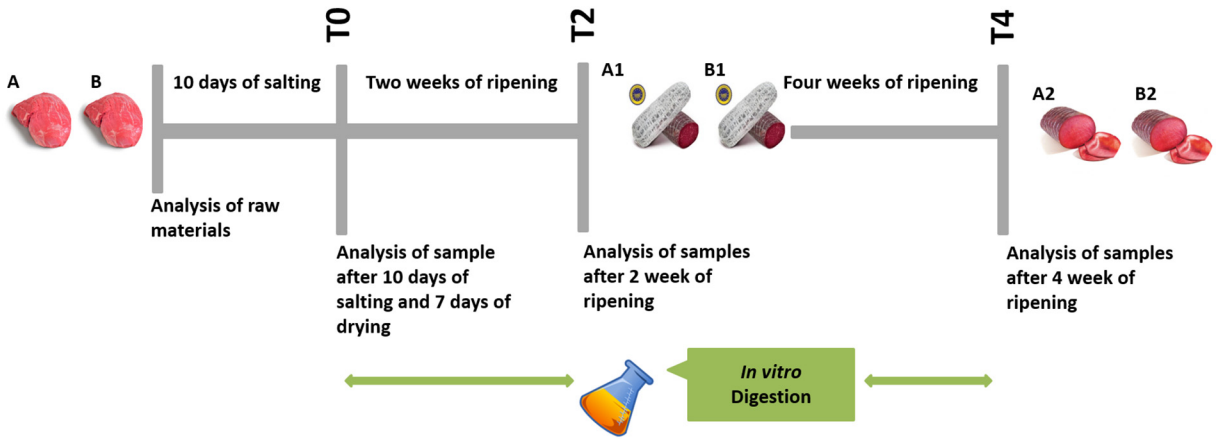

Fig. 1. Overview of the experimental design. At the end of sampling, a total of fourteen digestions have been performed on Bresaola samples (A-B x 3-time points x 2 replicates) and controls (meat without enzyme, A-B).

1. Introduction

The "Bresaola Valtellina" (Bresaola) is a Protected Geographical Indication (PGI) food produced using raw beef meat in the Italian alpine area called Valtellina. The production process uses different muscular masses, especially haunc's tio (punta d'anca), which represents the loin without its adducting muscle. The processing steps of Bresaola follow severe rules, which guarantee the authenticity of the product and the respect for the traditional processing. According to these rules, the single piece of meat is initially dry salted. In the same time, wine, spices, sugar, nitrites and nitrates, and ascorbic acid can be added to. Salting lasts about 10 days and it is followed by drying (7 days), which allows a rapid dehydration of the product to about 60% (*w*/w) moisture. Then, the salted and dried Bresaola undergoes maturation at 12–18 °C for 4–8 weeks, after which it can be sold as a whole, in pieces or sliced, vacuum packaged or under modified atmosphere. Cured meat products are generally employed as a valuable protein source, due to the good percentage of bioavailable peptides and amino acids (Deniz, Mora, Aristoy, Candoğan, & Toldrá, 2016; Mora, Escudero, & Toldrá, 2016). Meat proteins are exposed to the action of a variegate portfolio of proteases and peptidases. As a matter of fact, proteolysis starts at post-mortem in muscle from beef and it involves the initial degradation of different proteins including both structural (*e.g.* actin, myosin heavy chain, and troponin T) and metabolic proteins (*e.g.* glycogen phosphorylase, creatine kinase, phosphopyruvate hydratase, myokinase, pyruvate kinase) (Lana & Zolla, 2016). Nonetheless, most of the proteolysis occurs upon the activities of the gastrointestinal enzymes during meat digestion. As a result, diverse low molecular weight (LMW) nitrogen compounds are potentially released from precursor proteins and made free to diffuse to the absorption sites at the gastrointestinal tract (Parada & Aguilera, 2007; Pineda-Vadillo et al., 2016). However, the digestion process is also modulated by the supra-molecular organization of meat product, a characteristic that, for instance makes raw or cooked meat actually different (Dauphas et al., 2005). Meat processing can deeply change the matrix organization and, therefore, the complex network of molecular interactions and the compartmentalization of nutrients. In this way, nutrient bioavailability and the final nutritional value of the meat product can be greatly modified. For these reasons, it is necessary to assess the actual changes in a meat product under processing procedures (for example thermal treatment, drying, ripening) on the final properties of food, including digestibility, antioxidant capacity and digestive enzyme inhibition. One of the therapeutic approaches to retard glucose absorption is the inhibition of carbohydrate digestive enzymes (Chiou, Lai, Liao, Sung, & Lin, 2018). For this reason, the search for food with inhibiting activity on amylolytic enzymes is increasing. In the last years, the research focused on the inhibiting activity elicited by some food-derived peptides (Gallego et al., 2018, b; Gallego, Mora, Hayes, Reig, & Toldrá, 2017; Gallego, Mora, & Toldrá, 2018; Mora, Bolumar, Heres, & Toldrá, 2017). Although many plant food-derived peptides have shown anti-diabetic activities, studies on the potential bioactivity of peptides from animal foods are very limited. Recently, many peptides have been reported to inhibit carbohydrate digestive enzymes such as α-amylase (EC 3.2.1.1) and α-glucosidase (EC 3.2.1.20) (Li-Chan, 2015; Marcone, Belton, & Fitzgerald, 2017). It is thus necessary, for the assessment of the quality of cured meat products, to study the real bioaccessibility and bioavailability of these molecules and their interaction with the food matrix, and the effect of meat curing on the digestion enzymes (Capozzi & Trimigno, 2015).

The aim of this work was to investigate these phenomena in Bresaola as a model of cured and salted raw meat. To this aim, samples of Bresaola were firstly *in vitro* digested and then investigated through various techniques including *in vitro* biological and chemical assays, proteomic and NMR spectroscopy approaches (Capozzi & Bordoni, 2013). SDS-PAGE and NMR spectroscopy are complementary techniques, since the disappearance of protein fragments from the SDS gel, due to their LMW (REF) (Weber & Osborn, 1969), prevent them to be stained and detected, while NMR is able to detect and quantify whatever soluble molecule (Laghi, Picone, & Capozzi, 2014). The final goal was to gain a holistic view on the effect of the maturation time and digestion process of Bresaola on the molecular profile, the bioaccessibility of nutrients, and some potential biological activities of the digestates.

2. Materials and methods

2.1. Bresaola samples

Bresaola samples were provided by one of the major producer located in Valtellina and consisted of two different pieces (named A and B, 800 g each) collected after they have been salted and dried (Time 0, T0). Samples of Bresaola belonging to the same batch were also collected after 2 weeks (Time 2, T2) and 4 weeks (Time 4, T4) of ripening, as depicted in Fig. 1. The gross composition (g/100 g) of the samples was: moisture 58.55 ± 0.38, protein (Nx6.25) 32.2 ± 1.6, fat 3.37 ± 28, ash 5.44 ± 0.13, NaCl 4.06 ± 0.14, carbohydrates < 0.1. No significant differences in gross composition were found among the diverse pieces collected at three sampling times. Bresaola samples were also assessed for texture and sodium dodecyl sulfate-polyacrylamide gel electrophoresis (SDS-PAGE) profiles.

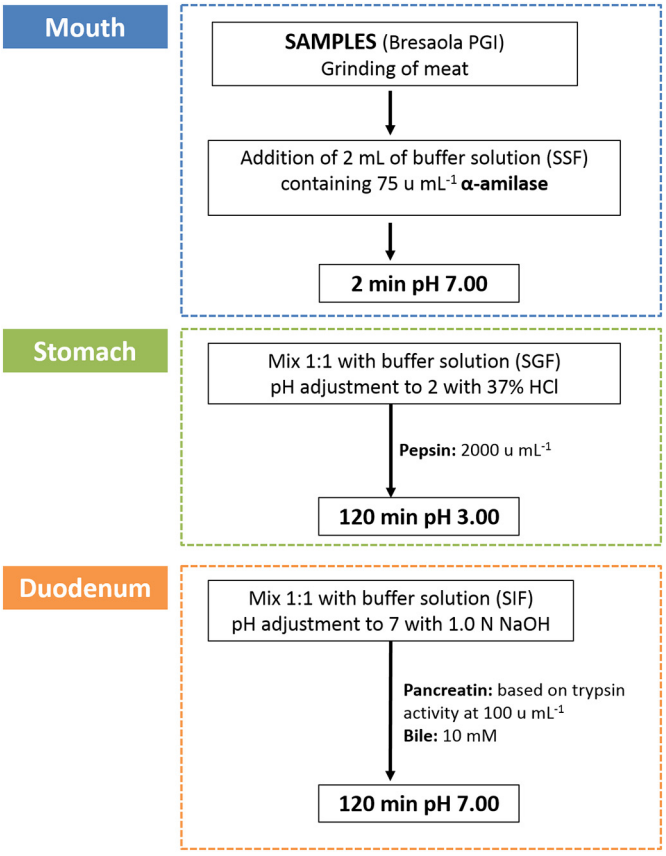

Fig. 2. Flow diagram of the INFOGEST *in vitro* digestion method. SSF, SGF and SIF are acronyms for Simulated Salivary Fluid, Simulated Gastric Fluid and Simulated Intestinal Fluid, respectively. Enzyme activities are in units per mL of final digestion mixture at each corresponding digestion phase (Minekus et al., 2014).

2.2. Texture profile analysis (TPA)

From each sample, slices 1.5 cm-thick were obtained by using an electric slicer. From the central part of each slice, two cylindrical cores were removed with a hand-coring device (diameter 2.2 cm). TPA was performed on the cylindrical cores at room temperature, using a 3365 Instron Universal Testing Machine (Instron Division of ITW Test and Measurement Italia S.r.l., Trezzano sul Naviglio, Italy) equipped with a 100 N load cell. Samples were compressed twice, to 50% of their original height, with a cross head speed of 200 mm/min (Van Schalkwyk, McMillin, Booyse, Witthuhn, & Hoffman, 2011) using a circular plate of 8 cm diameter. Hardness (N), chewiness (mJ), cohesion energy (ratio) and springiness (mm) were calculated according to Bourne (1978).

2.3. In vitro static gastrointestinal digestion

In this study, the standardized static *in vitro* digestion method, which has been proposed by the COST FA1005 Action INFOGEST was used (Minekus et al., 2014). The applied digestion protocol is illustrated in Fig. 2.

In total, fourteen digestions were carried out, both with and without Bresaola as a control. Enzyme activities were determined using the enzyme assays recommended in (Minekus et al., 2014). The chemical composition of the digestive fluid, pH and residence periods were adjusted to mimic the physiological conditions. Samples were collected at the end of the gastric phase and at the end of the duodenal phase. After the gastric step, the pH was increased to 7.00 with 35% NaOH to prevent possible modifications induced by acidic conditions. At the end of intestinal phase, the digestates were acidified to pH 2.00 with 37% HCl to stop pancreatic hydrolysis and to avoid bias caused by different pH values. Samples were immediately snap-frozen in liquid nitrogen and later stored as at −80 °C before any further analysis. Moreover, samples were collected on separate digestion, each stopping at either gastric or intestinal phase. Samples were not taken from the same digestion experiement, as sampling would had changed the composition of the remaining heterogeneous mixture. Analyses of Bresaola digestates were also run on their < 10-kDa fraction obtained by ultrafiltration of the whole digestate through Microcon-10 kDa Centrifugal Filter Unit with Ultracel-10 membrane (Merck Millipore, Darmstadt, Germany). In detail this fraction was studied for antioxidant capacity, α-aminoglucosidase and α-glucosidase inhibitory activity, SDS-PAGE and size exclusion HPLC patterns, and protein, peptide and metabolite profiles.

2.4. α-Amylase and α-glucosidase inhibitory activity assays

The α-amylase inhibitory assay was performed according to the method described by Koh, Wong, Loo, Kasapis, and Huang (2009) and Yang et al. (2012) with slight modifications. The pancreatic α-amylase (Megazyme® *E*-AMGDF), potato starch (Sigma-Aldrich 18,727) solutions were used as active enzyme and substrate, respectively. The absorbance at 620 nm was measured by microplate reader (Thermo Scientific Varioskan Flash, Finland). The α-glucosidase inhibitory assay was performed according to a previously described method by Koh et al. (2009). Reaction substrate 4-nitrophenyl α-D-galactopyranoside (PNPG, Sigma-Aldrich N0877) (30 mM) was used. Acarbose was used as positive control and percentage of inhibitory activities of samples were calculated by using the Eq. (1). A curve of percentage inhibition against sample concentration was plotted with means. The concentration of the sample required to produce a 50% inhibition of the initial rate of reaction (IC50) was determined by GraphPad Prism 6.0.

$$Inhibition\,(\%) = 100 \times \frac{[(A_{control} - A_{control\ blank}) - (A_{sample} - A_{sample\ blank})]}{(A_{control} - A_{control\ blank})} \quad (1)$$

where: $A_{control}$, $A_{controlblank}$, A_{sample}, $A_{sampleblank}$ refer to absorbance reading of reaction mixture containing active enzyme and buffer, inactive enzyme and buffer, active enzyme and sample (inhibitor) and inactive enzyme and sample (inhibitor), respectively. The substrate was present in all mixtures.

2.5. 1,1-diphenyl-2-picrylhydrazyl (DPPH) and 2,2′-azinobis 3-ethylbenzothiazoline-6-sulfonate (ABTS) radical-scavenging activities

The antioxidant activity (AA) of each sample was assessed by DPPH and ABTS free radicals scavenging activities according to Brand-Williams, Cuvelier, and Berset (1995) and Re et al. (1999), respectively. The AA was calculated against a control and compared to a Trolox standard curve and the result was recorded as antioxidant standard Trolox (6-hydroxy-2,5,7,8-tetramethychroman-2-carboxylic acid equivalents, mmol TEAC/g).

2.6. Sodium dodecyl sulphate - polyacrylamide gel electrophoresis (SDS-PAGE)

The undigested Bresaola samples and their digestates after gastric and intestinal steps were submitted to SDS-PAGE in order to determine the approximate MW of proteins and peptides. Amersham ECL™ precast gels (12%, GE Healthcare Bio-Sciences Corp, Piscataway, USA) were used on an Amersham ECL™ box according to the manufacturer's instructions. Injected samples were normalized to a total protein concentration of 1 g/L (2 µL per sample) for all gels, according to the manufacturer's instructions, to achieve best visibility and separation of the proteins. Samples were prepared under reducing (with β-mercaptoethanol) conditions. Proteins were visualized by Coomassie blue

staining (Bio-Safe Coomassie Stain G-250, Bio-Rad). An Amersham Low MW Calibration Kit (14.4 to 97 kg mol^{-1}, GE Healthcare UK Limited, UK) was used as the MW standard.

2.7. Size-exclusion high-performance liquid chromatography (HPLC)

At the end of each digestive phase, the < 10 kDa fraction from the whole digestates was studied by size exclusion HPLC. The MW distribution profiles of samples were estimated using a series connection column with TSK G 2000 SW (7.5 mm, 60 cm, 10 m, 131 Japan) fitted to a TSK guard column (7.5 mm, 7.5 cm). Twenty μL of samples were injected at the concentration of 2.5 g/L. A solution of 30% acetonitrile in 0.1% Trifluoroacetic acid (TFA) Milli-Q water was used as the eluent at a flow rate of 0.5 mL min^{-1}. Absorbances were monitored at 214 nm. Seven standards were used bovine Blue Dextran (2000 kDa), Carbonic anhydrase (29 kDa), β-lactoglobulin (18.276 kDa), Bacitracin (1.423 kDa), Leu-Try-Met-Arg (604.77 Da), Asp-Glu (262.22 Da), L-Leucine (131.22 Da), as MW calibration standards (log MW = −0.1508× + 8.61, with retention time, expressed in minutes, R2 = 0.9697). All samples were filtered through a low protein-binding Acrodisk® syringe filter (Pall Corporation, Port Washington, NY, USA) prior to injection onto the column.

2.8. Peptide analysis

Mass Spectrometry (MS) analysis was performed as previously described by Kopf-Bolanz et al. (2012) and Egger et al. (2017). The peptides present in the < 10 kDa fraction of the whole digestates were separated on a Rheos 2200 HPLC (Flux Instruments, Switzerland) equipped with a XTerra MS C18 column (3.5 μm, 1.0 mm × 150 mm, Waters). The HPLC was directly coupled to a linear ion trap mass spectrometer (LTQ, Thermo Scientific, Switzerland) using an ESI interface.

The mass spectrometer used is not a high resolution instrument, required to accurately quantify individual peptides, but it is ideally suited to get a general overview over the peptide patterns. Indeed, as peptides follow very well-known and specific fragmentation rules, high resolution instrument are not necessary for such identifications, and the amino acid counting method is fully based on identifications of peptides followed by amino acids counting in the identified peptide. The applied "amino acid counting" method was developed for covering the tests for reproducibility and physiology of the harmonized INFOGEST *in vitro* digestion method (Bohn et al., 2017; Egger et al., 2016; Egger, Schlegel, et al., 2017).

The samples were measured in multiple overlapping narrow mass windows spanning a m z^{-1} between 100 and 1300, and all raw files were merged for an identification search with Mascot (Matrix Science), using a database containing the major beef meat proteins. The database is homemade and it is maintained manually. It contains 69 milk proteins from different origin. The search engine parameters were set as follows: instrument configuration ESI-trap, consideration of average masses, peptide charge 1+, 2+, 3+, enzyme: none, variable peptide modifications were pyro-glutamic acid formation at N-terminal Glutamine (Gln), phosphorylation of serine and treonine, and possible methionine oxidation. MS/MS tolerance was set at 0.8 Da. To visualize the peptide abundance, individual amino acids within the identified peptides from the above mentioned meat proteins were summed up and a color code was applied (Egger, Schlegel, et al., 2017). The amino acid counting was performed with a home built Perl script extending Mascot (Matrix Science, London, UK) search engine, the color codes were adjusted using Microsoft Excel. The colors range from green to red, indicating low and high recurrence of specific amino acids, respectively. Unidentified protein sequences are shown as white stretches. The colors were normalized to the maximal number of identifications within the corresponding protein and digestion phase (Egger et al., 2017).

2.9. Proteomic analysis

Two-dimensional electrophoresis and spot excision and processing for proteomic analysis were carried out as previously reported (Ferranti et al., 2014). Protein spots hydrolyzed with trypsin were analyzed by MALDI TOF MS using a Voyager DE-Pro spectrometer (PerSeptive BioSystems, Framingham, MA) equipped with an N_2 laser (λ = 337 nm), using α-cyano-4-hydroxy-cinnamic acid as matrix (10 mg/mL in 50% acetonitrile, *v*/v, containing 0.1% TFA). Mass spectra were acquired in the reflector positive ion mode using the Delay Extraction (DE) technology. The accelerating voltage was 20 kV. External mass calibration was performed with a commercial mixture of standard peptides (PerSeptive Biosystems, Framingham, MA). A resolution of ≥8.000 was calculated in the working mass range. Raw data were analyzed using the Data Explorer 4.0 software furnished with the spectrometer. Post-source decay (PSD) MS analysis was carried out after isolation of the precursor ions using a timed ion selector set at an ion gate width of 1 Da. The PSD mass spectra were divided into seven segments; the laser power and the guide wire voltage were varied for each segment to optimize fragmentation and data collection. Approximately 200 laser shots were acquired for each segment. Fragmented ions were refocused onto the final detector by stepping down the voltage applied to the reflector. Finally, the individual segments were stitched together using the software purchased with the instrument. Peptide mass fingerprinting (PMF)-based identifications were carried out interrogating the National Center for Biotechnology Information (nrNCBI) and Swiss-Prot/TrEMBL databases (downloaded on November 2017) with Mascot (Matrix Science, London, UK) and Protein Prospector MS-FIT (http://prospector.ucsf.edu/) search engines. Mass tolerance of 0.3 Da, fixed carbamidomethylation of cysteines, variable pyro-glutamic acid formation at N-terminal Gln and possible methionine oxidation were set as search parameters. Up to one missed tryptic cleavage was accepted. Searches were taxonomically restricted to *Bos taurus*, whose genome has been completely sequenced. Probability MOWSE scores were automatically calculated by the search engines; only protein candidates with a score higher than the random match region (p < .05%) were considered. A protein was considered confidently identified based on at least four sequenced peptides. The identification of top scores of protein candidates was validated by manual peptide mass mapping.

2.10. ^{1}H nuclear magnetic resonance (^{1}H NMR) spectroscopy

Nuclear Magnetic Resonance has been employed in order to have a wide view of the molecular profile of samples during each digestion step. Samples were prepared for ^{1}H NMR according to Bordoni et al. (2014) by adding to 1 mL of each sample 160 μL of 100 mM phosphate buffer in deuterium oxide (D_2O), containing 10 mM 3-trimethylsilylpropanoic-2,2,3,3-d4 acid sodium salt (TMSP, Cambridge Isotope Laboratories) as an internal standard. After adjusting the pH to 7.00, the samples were centrifuged at 18,630*g* for 5 min in order to further remove impurities. All ^{1}H NMR spectra were recorded at 300 K on a Bruker US+ Avance III spectrometer operating at 600 MHz, equipped with a BBI-z probe and a B-ACS 60 sampler for automation (Bruker BioSpin, Karlsruhe, Germany). The spectra were collected with a 90° pulse of 14 μs with 10 W of power, a relaxation delay of 5 s and an acquisition time of 2.28 s. The spectra were registered by means of the first increment of a nuclear overhauser effect spectroscopy pulse sequence (NOESY), designed to suppress the residual signal of the solvent, while giving, for each proton, peaks proportional to the concentration of the substance they belong (Savorani et al., 2010).

Spectra were referenced to the TMSP signal at 0.00 ppm, solvent signal and noise were removed from the spectrum and the matrix was aligned with reference to the signal of lactate, also employed as a signal for normalization. The spectra of the blanks, *i.e.* the digestive enzymes, were also acquired and subtracted from the spectra of the digested

samples, in order to remove signals belonging just to the digestive components added according to the INFOGEST protocol. For not-digested samples, the changes occurring in the concentration of soluble, bioaccessible protein-derived fragments, during the ripening time, was calculated integrating the area of selected regions of the spectra, appropriately chosen for their informative power (Eq. (2)): total spectrum, aromatic region (6.00–7.85 ppm), alpha region (3.60–5.00 ppm), amides region (7.90–9.00 ppm), gamma-1 region (0.72–1.10 ppm), and gamma-2 region (0.56–0.72 ppm). The differences due to ripening, recorded between T0 and T2 (R2) and between T0 and T4 (R4), as the average and standard deviation among three replicates, are then used as proxies of the ripening effect on the bioaccessibility of protein-derived molecules as it is before digestion.

$$R2 = (A_{T2} - A_{T0})/(A_{T2})*100 \text{ or } R4 = (A_{T4} - A_{T0})/(A_{T4})*100 \quad (2)$$

where R2 is the differences recorded between T0 and T2, and R4 is the differences recorded between T0 and T4; A_{T0} is the area of the selected spectral region for not-digested sample at T0, A_{T2} is the area for not-digested sample at T2 and A_{T4} is the area for not-digested sample at T4.

For the digested samples, instead, the combined effects of ripening and digestion on the bioaccessibility of protein-derived fragments, was calculated by subtracting the area of an undigested sample (*e.g.*, A_{T0}) to that of the corresponding digested one (A'_{T0}), for each time-point (Eq. 3), thus considering the spectra of not-digested Bresaola as the baseline:

$$D0 = (A'_{T0} - A_{T0})/(A_{T0})*100 \text{ or } D2 = (A'_{T2} - A_{T2})/(A_{T2})*100 \text{ or } D4 = (A'_{T4} - A_{T4})/(A_{T4})*100 \quad (3)$$

where D0 is the digestion outcome recorded at T0, D2 is the one recorded at T2 and D4 is the one recorded at T4; A'_{T0} is the area of digested sample at T0, A'_{T2} is the area of digested sample at T2 and A'_{T4} is the area of digested sample at T4.

This calculation was applied to each spectral region listed above.

2.11. Statistical analysis

Results obtained from the different samples were compared by one-way analysis of variance (ANOVA), followed by the Least Significant Difference (LSD) test in order to evaluate significant differences among the averages (Statgraphics Plus 5.1, Statistical Graphics Corp., Herndon, VA, USA).

3. Results and discussion

3.1. Texture profile analysis (TPA)

The samples were firstly assessed for uniformity in macroscopic structural properties by TPA. At T0, the studied rheological parameters were not totally homogeneous among different Bresaola samples. Nonetheless, upon ripening, the same rheological properties tended to be more uniform among samples and no significant differences were observed among A and B batches after 4-week (T4) maturation (Table 1). Sometimes also replicates within the same batch showed relatively high standard errors. This finding is quite common for mechanical parameters of meat product, due to the complex structure of the matrix and to the different location of samples in the muscular mass (Barbut, 2014). Overall, with the exception of springiness, all the other evaluated parameters tended to decrease with ripening.

Table 1
Rheological parameters of Bresaola samples at the three-time points as assessed by TPA (values are mean of triplicates ± SE).

Maturing time (T), sample	Hardness (N)	Chewiness (mJ)	Cohesiveness (−)	Springiness (mm)
T0, A	24.9 ± 4.2^{a}	86.5 ± 12.8^{a}	0.46 ± 0.04^{b}	7.1 ± 0.2^{b}
T0, B	42.4 ± 4.6^{b}	86.4 ± 13.8^{a}	0.31 ± 0.04^{a}	6.2 ± 0.2^{a}
T2, A	20.5 ± 1.2^{a}	48.2 ± 3.4^{b}	0.31 ± 0.02^{b}	6.2 ± 0.1^{b}
T2, B	19.6 ± 1.1^{a}	42.5 ± 3.0^{b}	0.29 ± 0.02^{b}	6.0 ± 0.1^{ab}
T4, A	22.0 ± 1.9^{a}	45.5 ± 4.5^{a}	0.28 ± 0.02^{a}	6.6 ± 0.2^{a}
T4, B	25.7 ± 1.7^{a}	51.9 ± 4.0^{a}	0.27 ± 0.02^{a}	6.3 ± 0.1^{a}

a,b for the same variable, different superscript capital letters mean significant differences among different batches of each sample ($p < .05$).

3.2. In vitro inhibiting activity on amylolytic enzymes and antioxidant activity

In the present study, the inhibitory activities of Bresaola samples on these two enzymes were determined using the < 10-kDa fraction of the *in vitro* gastric digestates. Irrespective of the Bresaola maturation time, all the gastric digestates displayed significant ($p < .05$) inhibition of α-amylase in a concentration-dependent manner (Table 2). Meanwhile, IC50 of the standard compound acarbose at the same concentration used in the test was 1.26 (μg mL^{-1}). The peptidic fraction with MW < 10-kDa likely accounted for the revealed inhibitory activity (Mine, Li-Chan, & Jiang, 2011). This fraction is potentially less susceptible to further digestion by intestinal proteases and might had exerted an inhibitory effect on this carbohydrate digestive enzyme. In the α-glucosidase inhibition assay, the gastric digestates of samples at different maturation times displayed 50% inhibition activity at the given concentrations compared with acarbose (Table 2). Inhibition of α-amylase increased significantly with the time of sample maturation, but this was not observed for α-glucosidase inhibition (Table 2). The DPPH scavenging activity of gastric digestates of samples at T2 and T4 were significantly ($p < .05$) higher than that of the T0 sample digestate (Table 2). Similar results were also obtained for ABTS scavenging activities. As found for enzyme inhibition, the peptidic fraction generated during gastric digestion of Bresaola likely accounted for the revealed antioxidant activity. Indeed, diverse peptides derived from meat proteins have been reported to elicit this kind of activity (Lafarga & Hayes, 2014). These peptides can be generated during meat processing and aging, and also during gastrointestinal digestion in human. Bauchart et al. (2006) found more bioactive peptides in 14 days aged meat compared to the fresh counterpart. These bioactive peptides present short sequences (2–20 amino acids) and low MW. Some peptides with specific sequences and MW < 3–10 kDa were reported in cured meat as DPPH and Ferric Reducing Antioxidant Power (FRAP) radical scavengers (Gallego et al., 2017; Mora, Escudero, Fraser, Aristoy, & Toldrá, 2014; Mora, Gallego, Reig, & Toldrá, 2017). Besides peptides, some bioactive compounds present in the meat such as lipoic acid, coenzyme Q-10, L-carnitine and glutathione could exert antioxidant activity against radicals (Gokhisar & El, 2015). The undigested Bresaola samples and their digestates at different *in vitro* digestion steps were submitted to SDS-PAGE in order to determine the approximate molecular weight (MW) of proteins and/or peptides. The obtained SDS-PAGE profiles of samples are reported in Fig. 3. According to the INFOGEST *in vitro* protocol (Minekus et al., 2014), sampled proteins and peptides were those released in the aqueous/saline simulated intestinal fluid, as protein digestion progressed. Briefly (Fig. 3), the first gel represents the initial Bresaola samples, the second and third gels represent the digestates at gastric and intestinal phases, respectively. The main difference that characterized the first gel depended on the inter-variance of Bresaola samples. For example, the band between 55 e 43 kDa is present in cured samples but not at time 0 (T0); the same holds also for other two bands between 43 and 34 kDa, *i.e.* troponin and fructose biphosphate aldolase (the different intensity of the three samples depends on a different destaining degree). Following the *in vitro* gastric digestion, the bands from 72 to 43 kDa showed the substantial degradation of some sarcoplasmic proteins. Simultaneously, polypeptides covering the 95–55 kDa range appeared, due to the partial breakdown of myosin heavy chain (MHC). Furthermore, the band at 43 kDa (that could be

Table 2
Inhibitory activities against α-glucosidase and α-amylase, and antioxidant capacities of Bresaola gastric *in vitro* digestates.

Samples	IC_{50} values to α- glucosidase inhibition (μg mL^{-1})	IC_{50} values to α- amylase inhibition (μg mL^{-1})	DPPH activity (mmol TE g^{-1})	ABTS activity (mmol TE g^{-1})
Time 0	107.65 ± 12.64[a]	6.20 ± 0.63[a]	11.6 ± 1.6[a]	79 ± 0.7[a]
Time 2	95.65 ± 2.73[a]	4.31 ± 0.62[b]	22.7.0 ± 0.6[b]	151 ± 2.0[b]
Time 4	97.34 ± 4.73[a]	3.04 ± 1.20[c]	31.90 ± 2.4[c]	244 ± 3.1[c]
Acarbose*	120.90 ± 0.90[b]	1.26 ± 0.30[d]	–	–

enolase) was more marked at T2 and T4 than at T0. As expected, all the bands present in the gel of substrates digestion with enzymes belonged to the digestion and solubilization of high MW (HMW) proteins and not to the enzymes (as the control with gastric enzymes and without substrates indicated, not shown). Indeed, in the other half of the gel the substrate's digestion without enzymes is shown. A T0 the band between 43 e 34 kDa and those between 26 e 10 kDa were absent at T2 and T4. The quantity of HMW proteins is lower in the matured products (*i.e.*, samples at T2 and T4) than at T0, because of typical autolysis mechanism that has an effect on the soluble proteins. Conversely, other bands that are present at all sampling times belong to autolysis resistant proteins, *e.g.* myoglobin. After the simulated intestinal digestion, the protein bands only belonged to digestion enzymes (as the control with intestinal enzymes and without substrates indicated, not shown). As expected, after 2 h of intestinal digestion all the HMW proteins were hydrolyzed. Overall, the simulated gastric phase of *in vitro* digestion contributed to a massive release of myofibrillar proteins from the muscle tissue, making them predominate the protein fraction at the final stage of simulated digestion. The comparison between the intestinal and gastric phases of the Bresaola digestion without enzyme figured out few differences in the observed bands as well as in their intensity. This could be due to the different proteins isoelectric point. To sum up, the SDS-PAGE allowed to identify both the difference due to the three matrices and due to the presence or not of enzymes, pointing out that ripening contributed to larger release of proteins upon digestion, than that occurring with only salted meat.

3.3. Size-exclusion HPLC

At the end of each digestive phase, the < 10 kDa fraction from the whole digestates was studied by size exclusion HPLC. Using this technique, it was possible to both quantify the percentage of soluble low MW (LMW) peptides (< 1500 Da) and to link the proteolytic digestion kinetics with the different Bresaola samples. As shown in Fig. 4, the three digested Bresaola samples exhibited very similar peptide patterns and no differences were detected between samples at T0, T2 and T4. It is interesting to note that the gastric digestion (GD) produces on average 22.5 ± 1.5% and 29.7 ± 0.8% of peptides smaller than 250 Da or in the size interval of 250 to 600 Da, respectively. Practically no (< 1%) peptides larger than 1500 Da were detected. Sample that underwent gastric followed by intestinal digestion (ID) showed a shift towards smaller peptides with 52.10 ± 1.43% of the soluble peptides being smaller than 250 Da. This MW corresponds to free amino acids, di and tri-peptides, all of which are bioaccessible and deemed absorbable in small intestine.

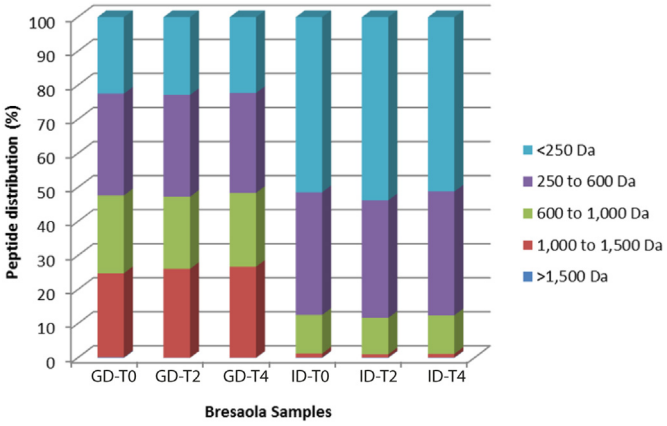

Fig. 4. Molecular weight distribution (in %) of digested Bresaola samples (< 10 kDa fraction of digestate), matured at T0, T2 and T4, after the gastric (GD) and intestinal (ID) digestion, as determined by size exclusion HPLC.

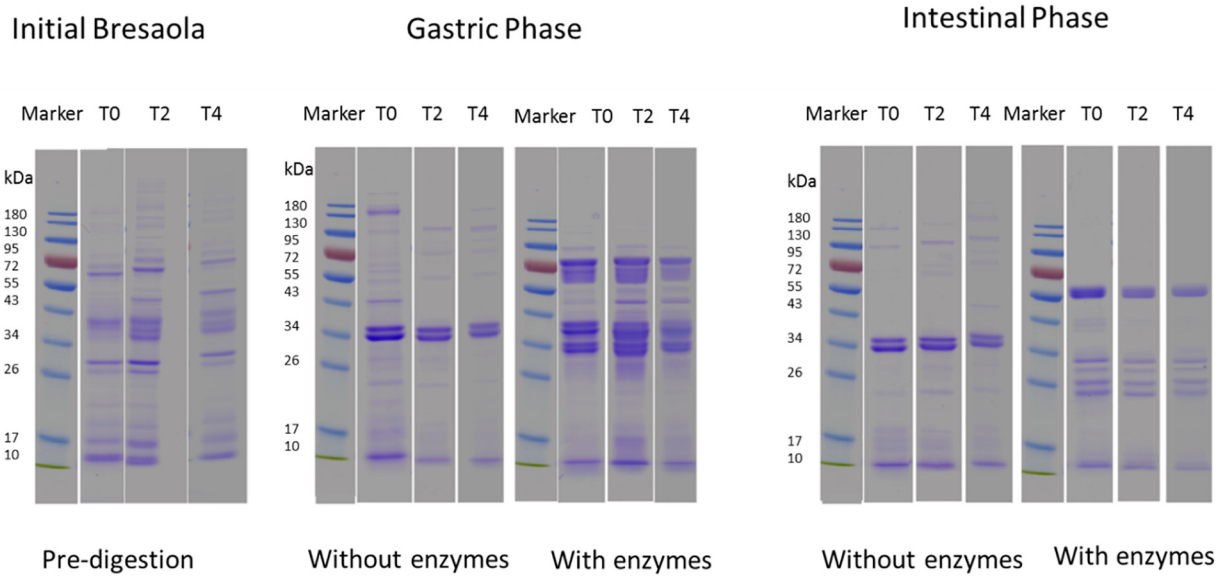

Fig. 3. SDS-PAGE of Bresaola samples at the three time-points, before and after digestive phases.

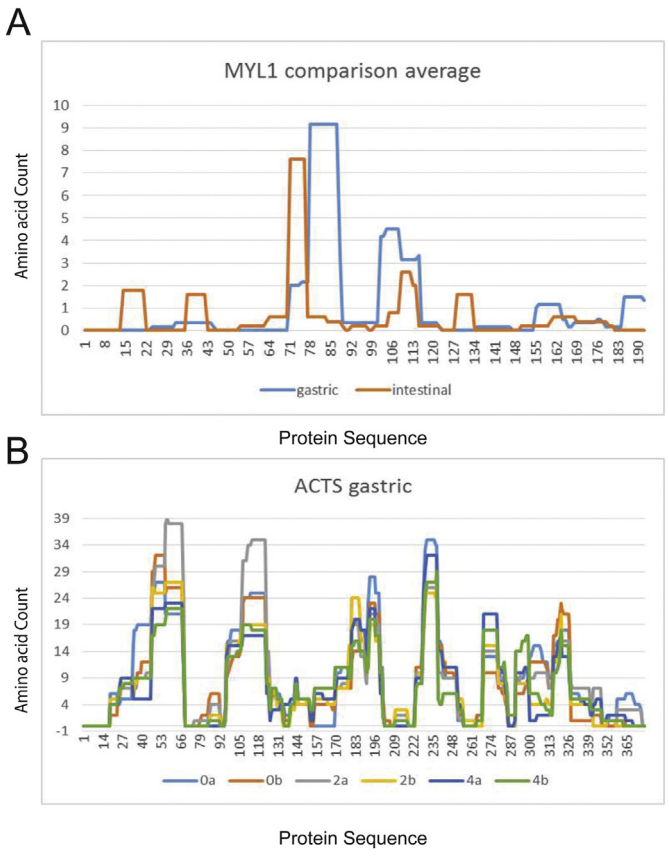

Fig. 5. A) The average peptide acid release of the MYL1 (myosin light) chain in the two digestive phases: gastric in blue and intestinal in orange. B) Comparison of different ripening times on peptide release on the example of ACTS. (For interpretation of the references to color in this figure legend, the reader is referred to the web version of this article.)

3.4. Peptide analysis

Peptides released from actin (ACTS), myosin-1 (MYH1), glyceraldehyde-3-phosphate dehydrogenase (G3P), myosin light chain (MYL1), myosin regulatory light chain (MLRS), beta-enolase (ENOB), creatine kinase M-type (KCRM), L-lactate dehydrogenase A chain (LDHA) were identified in Bresaola digestates. The abundance of each amino acid was measured and plots of the amino acid count in each digestive step, with or without the enzymes, were generated to investigate possible differences. Generally, more peptides are liberated in the gastric phase in the earliest time-points of ripening, whilst the opposite occurs in the intestinal phase, though within a lower extent, since most of the protein digestion was performed in the stomach.

A plot with the average of all the gastric results *versus* the average of all intestinal results was made to show how the different proteins are digested during the gastric and the intestinal phase. Some regions appear to be liberated only after intestinal digestion, whilst other regions appear more stable. For example, for MYL1 (Fig. 5A), it is clear how the gastric phase carries out most of the digestion, especially for bigger peptides, and releases more amino acids, whilst some smaller peptide regions released during the intestinal phase. Effect of different ripening times of Bresaola was tested on the example of ACTS (Fig. 5B). It was clearly shown that the ripening time has not a significant influence on the peptide pattern, although some differences in the relative abundance are appreciable. Indeed, the peptides corresponding to 50–65 in the ACTS sequence are more abundant at T2, whereas the peptides corresponding to 270–285 are more abundant at T4. The peptide release pattern was also studied on gastric samples without the enzyme action, to see if there was some release due to pH and the different time-

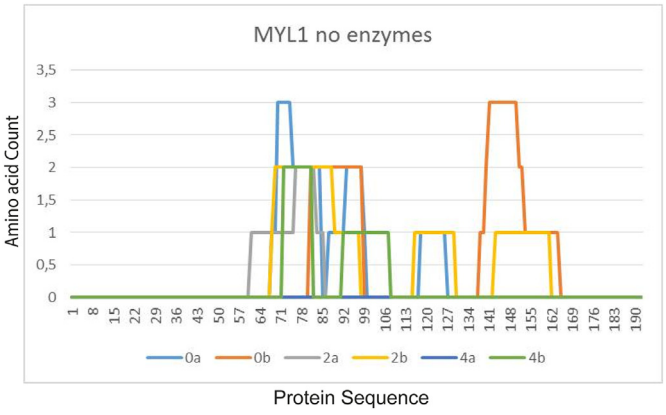

Fig. 6. Peptide release at the gastric phase for the two Bresaola samples (A and B) at T0, T2 and T4.

points in ripening. An example is shown in Fig. 6. It can be seen that only very low amount of peptides are present, when comparing to Fig. 5, showing the effect of digestion. Ripening itself has only marginal effect on initial occurrence of peptides.

3.5. Proteomic analysis

The effect of *in vitro* digestion was also evaluated by proteomic analysis carried out by combining 2D PAGE and MALDI-TOF MS. In Fig. 7 the analysis of Bresaola at T4 after *in vitro* digestion (Fig. 7A) is shown in comparison with a control consisting of the same sample incubated in the absence of enzymes (Fig. 7B). It can be seen that the main protein components of Bresaola that survived proteolysis, possibly because of their intrinsic structural stability were ACTS, tropomyosins, MHC fragments and myosin light chains. Furthermore, although more slowly than sarcoplasmic proteins, the myofibrillar ones were actually degraded by gastrointestinal proteases, as demonstrated by the occurrence of their fragments in the low MW peptide fraction (see Fig. 7A). Thus, simulated *in vitro* gastrointestinal digestion contributed to a massive release of myofibrillar proteins by the muscle tissue, making them predominate the protein fraction at the final stage of digestion (Sayd et al., 2018). These data are in agreement with previous studies

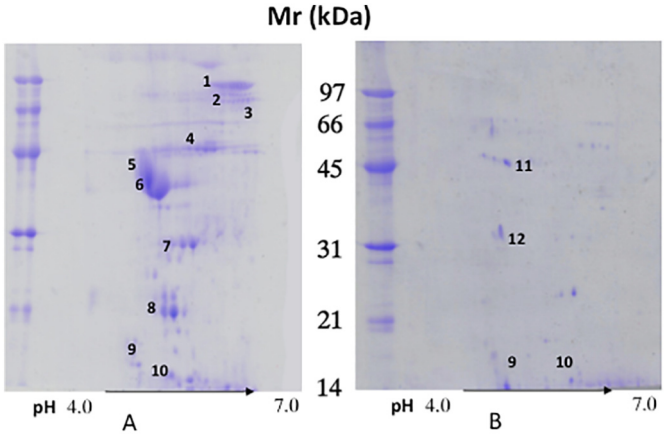

Fig. 7. 2DE-MS proteomic analysis of the simulated digest from the (A) digested Bresaola sample and (B) Bresaola control without enzymes. Identification of spots: 1: myosin heavy chain 1 (fragment); 2: Desmin; 3: serum albumin (theoretical MW/pI 66.4 / 5.84) + HSP 70; 4: actin (MW/pI 42.1 / 5.23); 5; 4: tropomyosin β-chain (MW/pI 33.3 / 4.62); 6: tropomyosin α-chain (MW/pI 33.3 / 4.62); 7: myosin light chain 1 (MLC1) (MW/pI 20.5 / 5.0); 8: myosin light chain 3, skeletal muscle isoform (MLC3F) (MW / pI 16.7 / 4.62); 9: myoglobin; 10: hemoglobin α-chain + hemoglobin β-chain; 11: phosphofructokinase + enolase; 12: fructose biphosphate aldolase.

Table 3
Changes in bioaccessibility consequent to ripening time for not-digested samples (C2 is the differences recorded on T0 and T2 and C4 is the differences recorded on T0 and T4).

	Gastric C2	Gastric C4	Intestinal C2	Intestinal C4
Total area	11.84 ± 0.14	10.99 ± 0.63	8.44 ± 2.14	7.97 ± 0.42
Aromatic region	9.43 ± 6.67	3.23 ± 3.01	3.21 ± 1.97	−5.98 ± −4.18
Alpha region	15.45 ± 2.81	14.40 ± 1.31	11.32 ± 1.73	8.71 ± 1.80
Amides region	−9.48 ± −4.79	−11.76 ± −5.52	7.80 ± 6.27	−9.57 ± −8.19
Gamma 1 region	30.86 ± 6.45	37.71 ± 16.48	8.27 ± 7.61	−13.47 ± −10.54
Gamma 2 region	11.67 ± 12.14	12.21 ± 5.49	12.80 ± 12.01	10.51 ± 6.38

Table 4
Changes in bioaccessibility consequent to ripening time plus digestion for digested samples (D0 is the differences recorded on T0, D2 is the differences recorded on T2 and D4 is the differences recorded on T4).

	Gastric D0	Gastric D2	Gastric D4	Intestinal D0	Intestinal D2	Intestinal D4
Total area	29.43 ± 9.83	26.06 ± 2.56	−20.89 ± −13.44	778.25 ± 121.26	845.08 ± 46.86	701.46 ± 230.57
Aromatic region	−36.13 ± −4.08	−30.80 ± −5.05	−30.61 ± −3.01	346.46 ± 51.70	346.23 ± 18.16	330.88 ± 97.75
Alpha region	−12.91 ± −8.10	−12.00 ± −3.23	−11.41 ± −0.90	178.1 ± 30.26	145.10 ± 5.76	135.07 ± 80.55
Amides region	−47.32 ± −8.85	−31.95 ± −4.85	3–5.04 ± −3.45	138.66 ± 40.54	197.81 ± 31.65	213.78 ± 71.58
Gamma 1 region	NI	NI	NI	919.21 ± 509.28	629.83 ± 80.39	1740.52 ± 567.22
Gamma 2 region	−14.64 ± −8.51	−11.87 ± −7.79	−22.55 ± −3.12	500.26 ± 178.25	532.83 ± 85.45	483.17 ± 201.85

(Ferranti et al., 2014) showing that meat proteins are in general highly digestible *in vitro*.

3.6. ^{1}H NMR spectroscopy

The acquired NMR spectra were investigated in order to assess the effect of maturation and digestion on release of soluble, bioaccessible protein-derived fragments in Bresaola samples.

The results are shown in Tables 3 and 4, reporting the changes in bioaccessibility consequent to ripening alone and ripening plus digestion, respectively. By looking at the ripening effects, the changes in bioaccessibility (Table 3) are much smaller than those observed for the digested samples (Table 4). The ripening alone is responsible for a slight increase of bioaccessibility (about 15%), more at gastric rather than at intestinal pH. The effect of pH on the matrix-solute interaction has been already demonstrated for the carnosine dipeptide (Marcolini et al., 2015). A special attention has to be paid to the decrement of the amide areas upon ripening which is explained by the increased solvent accessibility. Amide protons, when exchangeable with the solvent protons, are not detected in the normal NMR spectral region (7.90–9.00 ppm) but included in the water signal. Thus, for ripened samples, more hydrated proteins are expected and the signals of the corresponding water-accessible amide protons are lost, especially at lower pH. A large effect on the release of protein-derived fragments is obviously observed during digestion, more in the intestinal phase than in the gastric one. While excluding, for the above mentioned reason, the amide region, a large 10 fold increase is observed for the aromatic, alpha and aliphatic protons in the intestinal phase. Thus, mainly during the duodenal phase, molecules are liberated from the matrix by enzyme action and can, therefore, be available for further hydrolysis and absorption. In the intestinal phase, samples at the different ripening stages showed areas not significantly different from T0.

4. Conclusions

In conclusion, the results obtained by the proteomic study demonstrated that *in vitro* gastrointestinal digestion contributed to a considerable release of myofibrillar proteins by the muscle tissue, making them the predominant protein fraction at the end of digestion of Bresaola samples. Data from peptidomic and size exclusion HPLC assays demonstrated that the *in vitro* digestion degraded proteins of muscle tissue to medium-small peptides. In general, peptides were liberated with higher relative abundance in the gastric phase, during the digestion of samples at the earliest time-points of maturation. The proteolytic phenomena proceeded during the intestinal phase at the end of which peptides smaller than 250 Da represented half of the soluble peptides being present in the digestates. The released peptides were likely responsible for the inhibitory activity on amylolytic enzymes and for the antioxidant properties elicited by the gastric digestates of Bresaola. To have an absolute quantification of protein-derived molecules, NMR spectroscopy and SDS-PAGE analysis were carried out. NMR was able to follow the protein hydrolysis also in the late phases of digestion and appreciate the tenfold release of bioaccessible protein-derived molecules during the intestinal phase of the *in vitro* digestion, conversely not quantified by proteomic and peptidomic assay. Overall, the results demonstrated the negligible role of ripening in making the amount of meat proteins bioaccessible, whereas they confirmed the highly *in vitro* digestibility of meat proteins from Bresaola. However, the inhibition of α-amylase and the DPPH scavenging activity increased significantly with the time of sample maturation, thus demonstrating the sequence-specific nature of the released peptides depending on ripening.

This study represents a new approach merging proteomics and NMR spectroscopy to evaluate the effect of ripening and *in vitro* digestion on the bioaccessibility of proteins and peptides of meat products, and correlate the digestion process to the extent of their bioactivity.

Acknowledgements

The authors participate in the COST action FA1005 INFOGEST (http://www.cost-INFOGEST.eu/).

Conflicts of interest

The authors declare no conflict of interest.

References

Barbut, S. (2014). Texture. In F. Toldrá, Y. H. Hui, I. Astiasarán, J. G. Sebranek, & R. Talon (Eds.). *Handbook of Fermented Meat and Poultry* (pp. 207–2015). John Wiley & Sons, Ltd.

Bauchart, C., Rémond, D., Chambon, C., Patureau Mirand, P., Savary-Auzeloux, I., Reynès, C., & Morzel, M. (2006). *Small peptides (< 5kDa) found in ready-to-eat beef meat. 74*, 658–666.

Bohn, T., Carriere, F., Day, L., Deglaire, A., Egger, L., Freitas, D., Golding, M., Le Feunteun, S., Macierzanka, A., & Menard, O. (2017). Correlation between in vitro and in vivo data on food digestion. What can we predict with static in vitro digestion

models?, 1–23.
Bordoni, A., Laghi, L., Babini, E., Di Nunzio, M., Picone, G., Ciampa, A., ... Capozzi, F. (2014). *The foodomics approach for the evaluation of protein bioaccessibility in processed meat upon in vitro digestion. 35*, 1607–1614.
Bourne, M. C. (1978). *Texture profile analysis. 32*, 62–66.
Brand-Williams, W., Cuvelier, M.-E., & Berset, C. (1995). *Use of a free radical method to evaluate antioxidant activity. 28*, 25–30.
Capozzi, F., & Bordoni, A. (2013). *Foodomics: a new comprehensive approach to food and nutrition. 8*, 1.
Capozzi, F., & Trimigno, A. (2015). 11 - using metabolomics to describe food in detail. In L. Brennan, & J. L. Sebedio (Eds.). *Metabolomics as a Tool in Nutrition Research* (pp. 203–229). Woodhead Publishing.
Chiou, S. Y., Lai, J. Y., Liao, J. A., Sung, J. M., & Lin, S. D. (2018). *In vitro inhibition of lipase, α-amylase, α-glucosidase, and angiotensin-converting enzyme by defatted rice bran extracts of red-pericarp rice mutant. 95*, 167–176.
Dauphas, S., Mouhous-Riou, N., Metro, B., Mackie, A. R., Wilde, P. J., Anton, M., & Riaublanc, A. (2005). The supramolecular organisation of β-casein: Effect on interfacial properties. *19*, 387-393.
Deniz, E., Mora, L., Aristoy, M.-C., Candoğan, K., & Toldrá, F. (2016). *Free amino acids and bioactive peptides profile of Pastırma during its processing. 89*, 194–201.
Egger, L., Ménard, O., Baumann, C., Duerr, D., Schlegel, P., Stoll, P., ... Portmann, R. (2017). *Digestion of milk proteins: Comparing static and dynamic in vitro digestion systems with in vivo data.* https://doi.org/10.1016/j.foodres.2017.12.049.
Egger, L., Ménard, O., Delgado-Andrade, C., Alvito, P., Assunção, R., Balance, S., Barberá, R., Brodkorb, A., Cattenoz, T., & Clemente, A. (2016). The harmonized INFOGEST in vitro digestion method: From knowledge to action. *88*, 217-225.
Egger, L., Schlegel, P., Baumann, C., Stoffers, H., Guggisberg, D., Brügger, C., ... Portmann, R. (2017). *Physiological comparability of the harmonized INFOGEST in vitro digestion method to in vivo pig digestion.* https://doi.org/10.1016/j.foodres.2017.09.047.
Ferranti, P., Nitride, C., Nicolai, M. A., Mamone, G., Picariello, G., Bordoni, A., ... Capozzi, F. (2014). *In vitro digestion of Bresaola proteins and release of potential bioactive peptides. 63*, 157–169.
Gallego, M., Mora, L., Escudero, E., & Toldrá, F. (2018). *Bioactive peptides and free amino acids profiles in different types of European dry-fermented sausages. 276*, 71–78.
Gallego, M., Mora, L., Hayes, M., Reig, M., & Toldrá, F. (2017). *Effect of cooking and in vitro digestion on the antioxidant activity of dry-cured ham by-products. 97*, 296–306.
Gallego, M., Mora, L., & Toldrá, F. (2018). *Characterisation of the antioxidant peptide AEEEYPDL and its quantification in Spanish dry-cured ham. 258*, 8–15.
Gokhisar, O. K., & El, S. N. (2015). *Impacts of different cooking and storage methods on the retention and in vitro bioaccessibility of l-carnitine in veal muscle (M. longissimus dorsi). 240*, 311–318.
Koh, L. W., Wong, L. L., Loo, Y. Y., Kasapis, S., & Huang, D. (2009). *Evaluation of different teas against starch digestibility by mammalian glycosidases. 58*, 148–154.
Kopf-Bolanz, K. A., Schwander, F., Gijs, M., Vergères, G., Portmann, R., & Egger, L. (2012). Validation of an in vitro digestive system for studying macronutrient decomposition in humans. *142*, 245–250.
Lafarga, T., & Hayes, M. (2014). *Bioactive peptides from meat muscle and by-products: Generation, functionality and application as functional ingredients. 98*, 227–239.
Laghi, L., Picone, G., & Capozzi, F. (2014). *Nuclear magnetic resonance for foodomics beyond food analysis. 59*, 93–102.
Lana, A., & Zolla, L. (2016). *Proteolysis in meat tenderization from the point of view of each single protein: A proteomic perspective. 147*, 85–97.
Li-Chan, E. C. (2015). *Bioactive peptides and protein hydrolysates: Research trends and challenges for application as nutraceuticals and functional food ingredients. 1*, 28–37.
Marcolini, E., Babini, E., Bordoni, A., Di Nunzio, M., Laghi, L., Maczo, A., ... Capozzi, F. (2015). *Bioaccessibility of the bioactive peptide carnosine during in vitro digestion of cured beef meat. 63*, 4973–4978.
Marcone, S., Belton, O., & Fitzgerald, D. J. (2017). Milk-derived bioactive peptides and their health promoting effects: A potential role in atherosclerosis. *83*, 152–162.
Mine, Y., Li-Chan, E., & Jiang, B. (2011). *Bioactive proteins and peptides as functional foods and nutraceuticals. Vol. 29*. John Wiley & Sons.
Minekus, M., Alminger, M., Alvito, P., Ballance, S., Bohn, T., Bourlieu, C., ... Dupont, D. (2014). *A standardised static in vitro digestion method suitable for food–an international consensus. 5*, 1113–1124.
Mora, L., Bolumar, T., Heres, A., & Toldrá, F. (2017). *Effect of cooking and simulated gastrointestinal digestion on the activity of generated bioactive peptides in aged beef meat. 8*, 4347–4355.
Mora, L., Escudero, E., Fraser, P. D., Aristoy, M.-C., & Toldrá, F. (2014). *Proteomic identification of antioxidant peptides from 400 to 2500 Da generated in Spanish dry-cured ham contained in a size-exclusion chromatography fraction. 56*, 68–76.
Mora, L., Escudero, E., & Toldrá, F. (2016). *Characterization of the peptide profile in Spanish Teruel, Italian Parma and Belgian dry-cured hams and its potential bioactivity. 89*, 638–646.
Mora, L., Gallego, M., Reig, M., & Toldrá, F. (2017). *Challenges in the quantitation of naturally generated bioactive peptides in processed meats*.
Parada, J., & Aguilera, J. M. (2007). Food microstructure affects the bioavailability of several nutrients. *72*, R21-R32.
Pineda-Vadillo, C., Nau, F., Dubiard, C. G., Cheynier, V., Meudec, E., Sanz-Buenhombre, M., Guadarrama, A., Tóth, T., Csavajda, É., Hingyi, H., Karakaya, S., Sibakov, J., Capozzi, F., Bordoni, A., & Dupont, D. (2016). In vitro digestion of dairy and egg products enriched with grape extracts: Effect of the food matrix on polyphenol bioaccessibility and antioxidant activity. *88*, 284-292.
Re, R., Pellegrini, N., Proteggente, A., Pannala, A., Yang, M., & Rice-Evans, C. (1999). *Antioxidant activity applying an improved ABTS radical cation decolorization assay. 26* (1231-l).
Savorani, F., Picone, G., Badiani, A., Fagioli, P., Capozzi, F., & Engelsen, S. B. (2010). *Metabolic profiling and aquaculture differentiation of gilthead sea bream by 1H NMR metabonomics. 120*, 907–914.
Sayd, T., Dufour, C., Chambon, C., Buffière, C., Remond, D., & Santé-Lhoutellier, V. (2018). *Combined in vivo and in silico approaches for predicting the release of bioactive peptides from meat digestion. 249*, 111–118.
Van Schalkwyk, D., McMillin, K., Booyse, M., Witthuhn, R., & Hoffman, L. (2011). *Physico-chemical, microbiological, textural and sensory attributes of matured game salami produced from springbok (Antidorcas marsupialis), gemsbok (Oryx gazella), kudu (Tragelaphus strepsiceros) and zebra (Equus burchelli) harvested in Namibia. 88*, 36–44.
Weber, K., & Osborn, M. (1969). *The reliability of molecular weight determinations by dodecyl sulfate-polyacrylamide gel electrophoresis. 244*, 4406–4412.
Yang, X.-W., Huang, M.-Z., Jin, Y.-S., Sun, L.-N., Song, Y., & Chen, H.-S. (2012). *Phenolics from Bidens bipinnata and their amylase inhibitory properties. 83*, 1169–1175.